NATIONAL ADVISORY COMMITTEE FOR AERONAUTICS

TECHNICAL NOTE 3197

MECHANICAL PROPERTIES AT ROOM TEMPERATURE OF FOUR CERMETS OF TITANIUM CARBIDE WITH NICKEL BINDER

By Aldie E. Johnson, Jr.

Langley Aeronautical Laboratory
Langley Field, Va.

Washington
August 1954

NATIONAL ADVISORY COMMITTEE FOR AERONAUTICS

TECHNICAL NOTE 3197

MECHANICAL PROPERTIES AT ROOM TEMPERATURE OF FOUR CERMETS OF TITANIUM CARBIDE WITH NICKEL BINDER

By Aldie E. Johnson, Jr.

SUMMARY

Room-temperature stress-strain curves are presented for compression, tension, and shear loadings on four compositions of titanium carbide with nickel binder. Values of ultimate strength, modulus of elasticity, modulus of rigidity, Poisson's ratio in the elastic region, density, and hardness for the four materials are tabulated.

INTRODUCTION

In recent years, carbide-type ceramic materials (combined with metals and called cermets or ceramals - see ref. 1) have been used to a limited extent in structural parts of aircraft, particularly for applications involving the high temperatures found in engine parts or turbine blades. The available data on the properties of cermets are limited and principally related to specific high-temperature applications. Some isolated data for room-temperature compressive strength and compressive modulus of elasticity are available, but data for room-temperature modulus of rigidity, Poisson's ratio, tensile strength, and, in particular, complete stress-strain curves are essentially nonexistent. Reference 2 provides a notable exception for one particular elevated-temperature material. The tests reported in reference 2 were of a material composed of about 80 percent titanium carbide and 20 percent nickel, but with the inclusion of a multiple carbide of columbium, tantalum, and titanium.

The high modulus of elasticity and high ratio of modulus to density for cermets suggests the possible use of some compositions in special wind-tunnel models, model supports, pilotless-aircraft research missiles, or other applications for which the primary requisites are high stiffness or high ratios of stiffness to weight. In order to provide information on the room-temperature mechanical properties for such applications, an investigation has been made of the pertinent properties in compression, tension, and torsional shear for some cermets with a titanium-carbide

base. Complete stress-strain curves to failure were obtained in addition to values of modulus of elasticity, modulus of rigidity, Poisson's ratio, ultimate strength, and density. The four materials tested were the following combinations of titanium carbide with nickel as a binder element:

TiC, percent	Ni, percent
95	5
90	10
80	20
70	30

The test specimens were fabricated at Kennametal, Inc., by the hot-pressing technique.

DESCRIPTION OF SPECIMENS AND TESTS

The sizes and shapes of the specimens are shown in figure 1; specimens 1, 2, and 3 are, respectively, compression, tension, and shear specimens. Two specimens of each of the four compositions were tested in each of the three loadings. The specifications for the surface finish of the specimens called for smooth grind and, in the case of the tensile specimens, an additional requirement of no transverse scratches visible with the naked eye and no longitudinal scratches exceeding 4 microinches in depth.

Inasmuch as the carbides are very hard and brittle, the experimental work of determining the mechanical properties, particularly the compressive strength, proved to be unusually difficult. Each of the three test-specimen shapes used in this investigation was designed especially for the material tested. The diameter and length of the test section of the tensile specimen corresponded to the proportions of standard round tensile specimens. The designs necessitated special grips and fixtures for the tension and torsion tests. The test specimens and testing techniques used are described in detail in subsequent sections.

The volumes and weights of the compression specimens were used to determine the densities of the various compositions and these are shown in table I. The hardness of the materials (given in table I) was determined from superficial hardness tests (Rockwell 30-N scale).

Compression Tests

The compression test specimen shown in figure 1 is a column 3 inches long and 1 inch square, with end surfaces ground flat, parallel, and perpendicular to the specimen axis. Compression was applied to the ends of the specimen through hardened tungsten-carbide bearing blocks by the Langley 1,200,000-pound-capacity testing machine. The testing-machine loads were measured with an error of less than 0.5 percent. Figure 2 shows a view of the specimen between the loading platens of the testing machine.

Three measurements were made in each compression test: elastic transverse strain, elastic longitudinal strain, and complete load-strain curve to failure of the specimen. The loading platen of the testing machine was adjusted for each test so that, at an elastic load corresponding to about 25 percent of the ultimate load on the specimen, equal strain (within ± 0.000005 for the pair of transverse gages and within ± 0.00001 for the longitudinal gages) was indicated by the pairs of gages on opposite faces of the specimen. The elastic transverse strains were measured on two opposite faces of the specimen at each load increment with Tuckerman optical strain gages. Coincidently with these measurements, the longitudinal strains on the remaining two faces of the specimen were measured with Baldwin SR-4 resistance-type wire strain gages (type AX-5), as a check on the alinement of the specimen during the test.

After the transverse strains had been determined, the load was removed from the specimen and the transverse gages were replaced by Tuckerman optical gages in the longitudinal direction. The alinement of the loading platen of the machine was checked (and corrected if necessary) to insure that the indicated longitudinal strains on pairs of opposite faces would be equal within the previously described limits. The elastic longitudinal strains were determined similarly to the elastic transverse strains, and wire strain gages on the remaining two faces were again used as a check on alinement and also to provide a continuous load-strain curve of the material to failure. The longitudinal optical gages were removed from the specimen at a load corresponding to the alinement load and the two wire strain gages were used to obtain the remainder of the load-strain curve. After removal of the optical gages, a protective shield was placed around the specimen, inasmuch as the collapse of the column specimen produced a shower of flying fragments of the material. Figure 2 shows the optical gages, the autocollimators for reading the gages, the wire strain gages, and part of the protective shield in back of the specimen.

Tension Tests

The tension test specimens had a test section 1/2 inch in diameter by $2\frac{1}{4}$ inches long and a fillet of 1-inch radius between the test section and the 40° (included angle) conical ends. The design of the test specimens is somewhat different from that of the specimens reported in reference 2 or other specimens tested by the National Advisory Committee for Aeronautics (see, for example, ref. 3) in that the present specimens had a larger cone angle and smaller fillet.

The tension specimens were held in special grips having hardened and ground spherical seats to help in alining the specimens for equal strain over the cross section. The tension bolts between the special grips and the testing-machine crossheads were also spherically seated in the crossheads. Figure 3 shows a tension specimen in the grips before the parts of the lower grip were screwed together. Figure 4 shows a cutaway view of the test specimen in the grips.

The surface of the test section was superfinished with 0 - $\frac{1}{2}$ micron size diamond compound to remove the transverse (circumferential) scratches which were a result of grinding the specimens to final shape. In some specimens, a few faint transverse scratches were left on the surface because of the prohibitive cost of removing them completely. The scratches, however, did not necessarily cause fracture of the specimens, inasmuch as failure occurred at other points along the test length.

Autographic load-strain curves were obtained from four Baldwin SR-4 wire strain gages (type A-5) spaced equally around the circumference of the test section. The specimens were adjusted in the grips so that, in the low elastic range of the material, the longitudinal strains measured at the four gage locations around the circumference of the specimen were equal within ± 0.00003. The testing-machine loads were measured with an error less than 0.5 percent.

Shear Tests

The shear test specimens were hollow cylinders of 1/8-inch wall thickness and $1\frac{1}{4}$-inch outside diameter. There was a fillet of 5/8-inch radius between the 2-inch-long test section and the hexagonal ends. The hexagonal ends were secured by wedges in special fixtures attached to the combined load testing machine of the Langley structures research laboratory and a torsional moment was applied while all other load components were held at zero. Figure 5 shows a view of the specimen and fixtures between the heads of the testing machine and figure 6 shows a cutaway view of the specimen in the test fixture.

Moment—shear-strain records were obtained to failure of the specimens. Two Baldwin wire strain gage rosettes (type AR-1) were used to determine the shear strains. The testing-machine loads were measured with an error less than 1 percent of the indicated load or less than 150 inch-pounds, whichever was greater.

RESULTS AND DISCUSSION

Stress-Strain Curves

Complete stress-strain curves (figs. 7 to 9) were obtained to the ultimate strength of each specimen. For the compression tests (fig. 7) the stress was determined as the load in the specimen P, divided by the original cross-sectional area of the specimen A, and the strains were obtained from optical and wire strain gages. The values of strain obtained from the two optical gages were averaged to determine the elastic portion of the stress-strain curve and the average of the two wire strain gages was used to determine the remainder of the curve. The compositions containing 80 percent titanium carbide and 70 percent titanium carbide exhibited sufficient ductility so that a yield stress σ_{cy} (0.2 percent offset) could be determined.

For the tension tests (fig. 8) the stress was determined as the P/A stress, and the strains were determined as the average of the strains obtained from the four wire gages. Although in all cases failure occurred before a yield stress corresponding to 0.2-percent offset was reached, for the composition containing 70 percent titanium carbide a strain of approximately 0.003 was achieved before failure.

For the torsion tests, the outer-surface shear strain γ_o was computed from the outer-surface compressive and tensile strains measured by the elements of the wire strain gage rosette at angles of 45° on either side of the longitudinal axis of the specimen. With the compressive direction taken as positive, the equation is

$$\gamma_o = \epsilon_1 - \epsilon_2$$

where

ϵ_1 compressive strain

ϵ_2 tensile strain

Thus, a torque—shear-strain curve was determined from the original torque-strain curves.

An expression for the outer-surface shear stress in a twisted hollow cylinder can be derived in a manner similar to that given in reference 4 for the case of a solid cylinder. The resulting equation is

$$\tau_o = \frac{1}{2\pi r_o^3}\left(\gamma_o \frac{dT}{d\gamma_o} + 3T\right) + \tau_i\left(\frac{r_i}{r_o}\right)^3$$

where

τ_o, τ_i shear stress at outer and inner surfaces, respectively

T applied torque

r_o, r_i outer and inner radii, respectively, of the cylindrical test section

The shear stress-strain curves were determined from this torque—shear-stress relation and the torque—shear-strain curves. In the elastic range, the torque-stress equation reduces to the familiar form

$$\tau_o = \frac{2T}{\pi r_o^3\left[1 - \left(\frac{r_i}{r_o}\right)^4\right]}$$

which may also be used in the inelastic stress range to determine an approximate relationship between applied torque and outer-surface shear stress. The approximate stress-strain curve determined from the elastic-stress—torque equation was then used, in conjunction with the general stress-torque equation, to calculate an improved stress-strain curve. For given values of torque, values of τ_i were read from the approximate stress-strain curve at values of strain compatible with the assumption that the shear strain varies linearly from the longitudinal axis of the cylinder to the outer surface, and values of τ_o were then determined from the general equation. Successively improved stress-strain curves were computed until convergence was obtained. The final shear stress-strain curves for the torsion specimens are given in figure 9.

Elastic Properties

The elastic properties determined for the four materials are modulus of elasticity E, modulus of rigidity G, and Poisson's ratio μ. These properties are given in table I and their variations with the composition of the material are shown in figure 10.

Table I gives both tensile and compressive values of modulus of elasticity, but, inasmuch as the tensile and compressive values are similar and the compressive values were determined with a higher degree of accuracy, the tensile test points have been omitted from figure 10. The highest modulus of elasticity is noted in the region of a composition of about 90 percent titanium carbide and 10 percent nickel. The scatter of the data precludes a similar conclusion for the modulus of rigidity obtained from the shear tests. It is evident from the values of modulus of elasticity and density that the ratios of modulus to density (given in table I) are 2 to 3 times higher than those for the common structural materials, which are in the range of 90,000 to 110,000 ksi/lb/cu in.

The present data for the compressive modulus of elasticity and Poisson's ratio were obtained with Tuckerman optical gages, which are considerably more accurate than wire strain gages in measuring strains. Inasmuch as the values of μ and E in compression were determined with greater precision than the values of G, which were obtained from wire-strain-gage data in the shear tests, the equation for an isotropic material,

$$G = \frac{E}{2(1 + \mu)}$$

was used with the experimental values of E and μ as a check on the experimentally determined values of G. The average values of E and μ for each composition were used to compute the values of G_{calc} given in table I and these values indicate a good correlation with the values of G determined from the torsion tests.

Strength

The compressive and tensile strengths were determined as the highest value of P/A stress in each test. The shear strengths were computed from the maximum moment and maximum shear strain as described in a previous section. These test data are given in table I.

In figure 11, curves have been faired through the test data to show the variation in ultimate strength for the three loadings in terms of the

composition of the material. The compressive strength appears to be highest for a composition containing between 10 and 20 percent binder material. The data indicate that increasing amounts of the nickel binder material improve the tensile and shear strengths.

A typical failure of a shear specimen is shown in figure 12 and indicates that the failure occurred along planes inclined approximately 45° to the longitudinal axis of the specimen. A failure typical of a compression specimen is shown in figure 13. An untested specimen is shown on the left for comparison. The wire strain gages are evident on the untested specimen and are also visible on pieces of the shattered specimen. The tensile failures were typical of brittle materials and occurred before any appreciable permanent strain was evident in the specimens. The location of the fracture with respect to the center of the $2\frac{1}{4}$-inch-long test section is given in table I.

CONCLUDING REMARKS

Room-temperature stress-strain curves are presented for compression, tension, and shear loadings on four different compositions of titanium carbide with nickel binder. Values of ultimate strength, modulus of elasticity, modulus of rigidity, Poisson's ratio in the elastic region, density, and hardness for the four materials are tabulated. The high values of compressive strength, modulus of elasticity, and particularly the high ratio of modulus to density indicate possible advantageous uses of the materials in special applications where the more common materials are not adequate and where suitable design precautions are taken with regard to the lack of ductility and the relatively low and variable tensile and shear strengths of these cermets.

Langley Aeronautical Laboratory,
National Advisory Committee for Aeronautics,
Langley Field, Va., April 6, 1954.

REFERENCES

1. Hoffman, Charles A., Ault, G. Mervin, and Gangler, James J.: Initial Investigation of Carbide-Type Ceramal of 80-Percent Titanium Carbide Plus 20-Percent Cobalt for Use as Gas-Turbine-Blade Material. NACA TN 1836, 1949.

2. Duckworth, W. H., Schwope, A. D., et al.: Mechanical Property Tests on Ceramic Bodies. AF Tech. Rep. No. 6512 (Contract No. AF 33(038)-8682, RDO No. R-605-233), Battelle Memorial Inst., Apr. 1951.

3. Kunen, Alfred E., Hartwig, Frederick J., and Bressman, Joseph R.: Tensile Properties of a Sillimanite Refractory at Elevated Temperatures. NACA TN 1165, 1946.

4. Nádai, A.: Theory of Flow and Fracture of Solids. Vol. I, second ed., McGraw-Hill Book Co., Inc., 1950, pp. 347-349.

TABLE I

PROPERTIES OF CERMETS COMPOSED OF TITANIUM CARBIDE WITH NICKEL BINDER

Composition		Density, lb/cu in.	Hardness, Rockwell 30-N scale	Poisson's ratio, μ	Modulus in —			Ultimate strength in —			Compressive yield stress, σ_{cy}, ksi	$\frac{\text{Modulus}}{\text{Density}}$, ksi / lb/cu in.	Tension fracture (a)	Modulus in shear, G_{calc}, ksi
TiC, %	Ni, %				Compression, E, ksi	Tension, E, ksi	Shear, G, ksi	Compression, σ_{max}, ksi	Tension, σ_{max}, ksi	Shear, τ_{max}, ksi				
95	5	0.171	88	0.18 .19	47.8×10^3 47.7	49.5×10^3 49.0	23.5×10^3 (b)	330 327	38.1 37.3	35.9 (b)		279×10^3 279	3/4 1/2	20.1×10^3
90	10	.178	88	.20 (c)	51.2 49.2	48.2 47.7	25.4 23.0	353 349	65.6 72.2	55.8 74.2		288 276	0 3/4	20.9
80	20	.190	84	.19 .19	50.6 49.7	46.7 45.7	25.8 22.4	350 351	74.2 77.6	88.9 95.0	286 299	266 262	[d] $1\frac{1}{4}$ [d] $1\frac{1}{4}$	21.1
70	30	.200	79	.22 .21	48.0 47.0	47.9 45.0	27.5 20.4	337 335	114.8 118.0	101.0 99.2	238 235	240 235	1/4 5/8	19.6

[a]Distance from fracture to center of test section, in.

[b]No test.

[c]Not measured.

[d]In fillet.

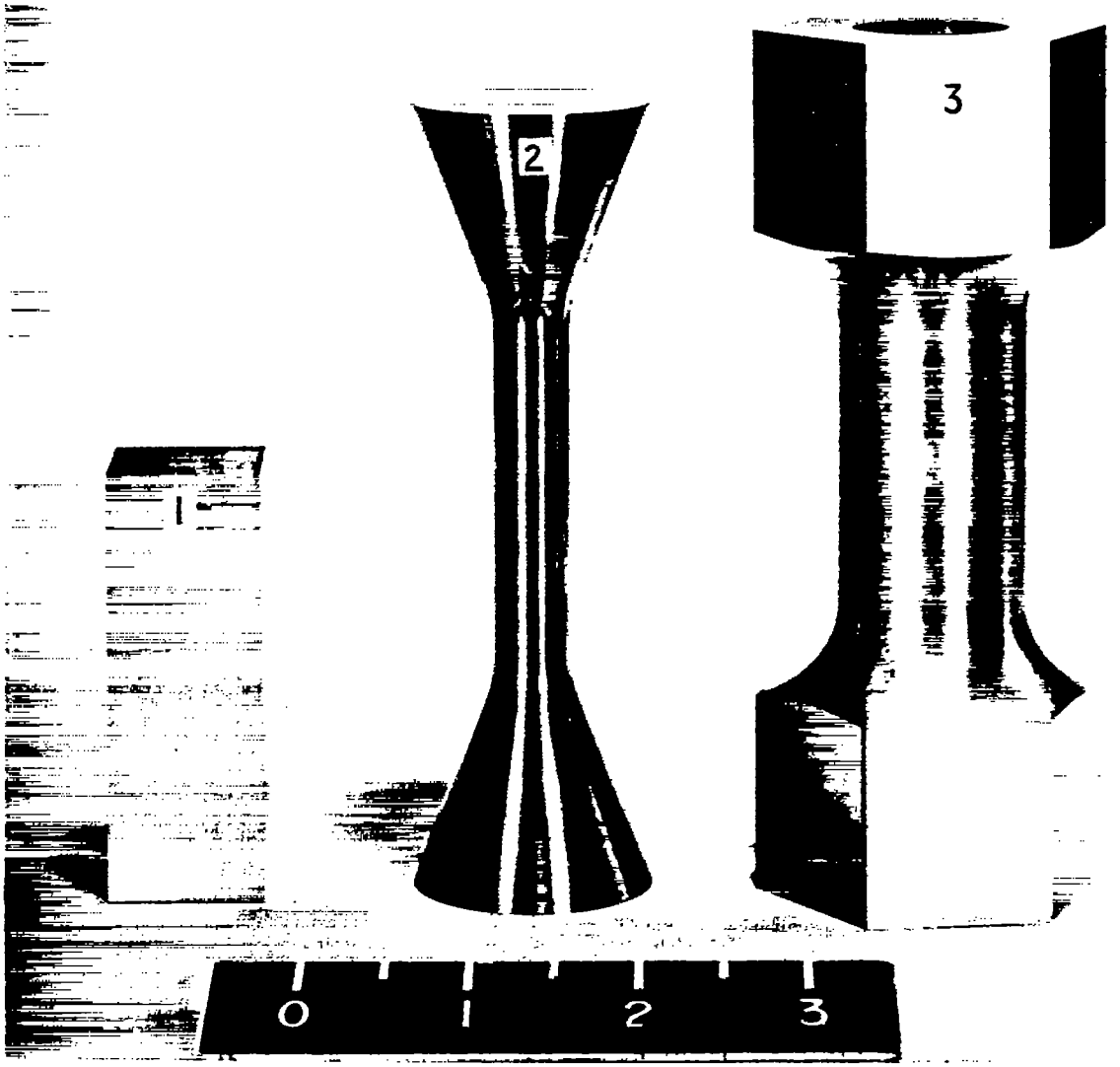

L-75396.1

Figure 1.- Compression, tension, and shear test specimens.

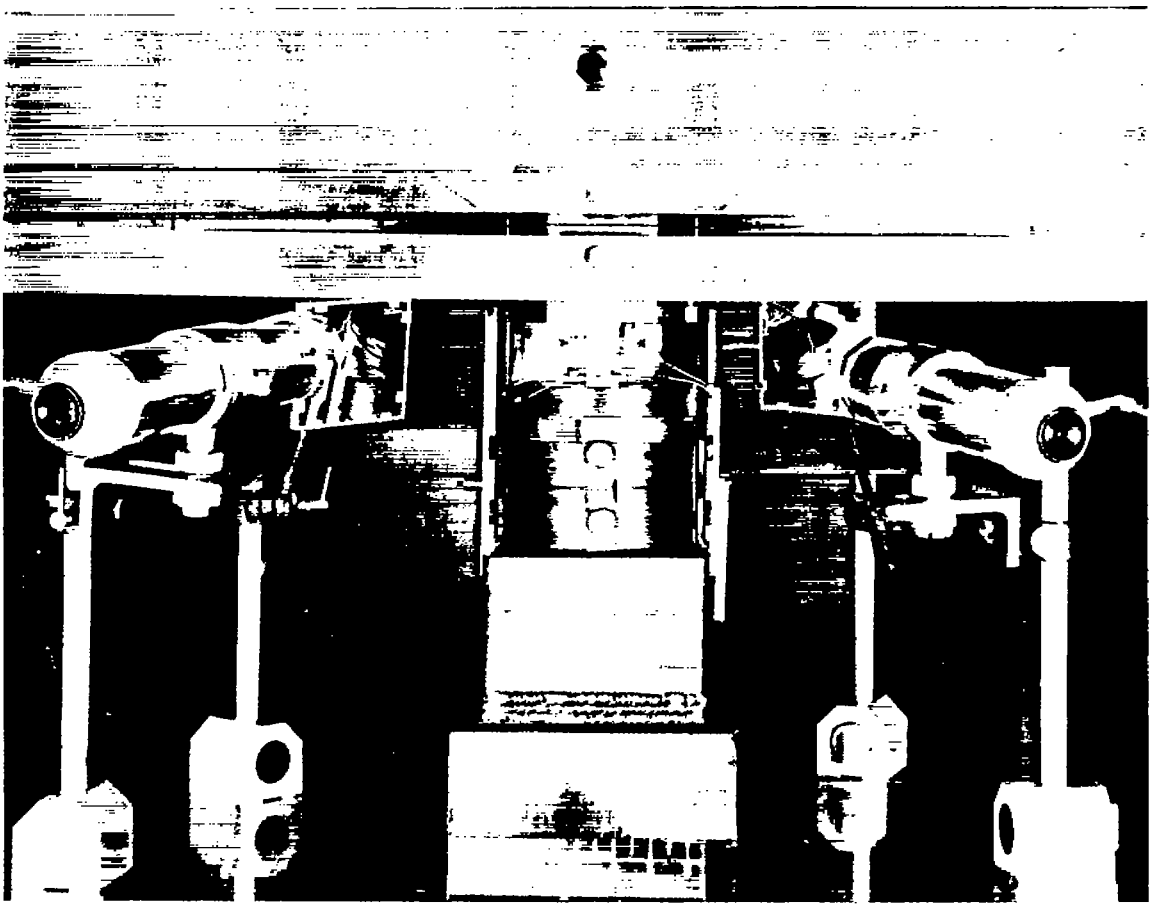

L-75521

Figure 2.— Compression-test setup.

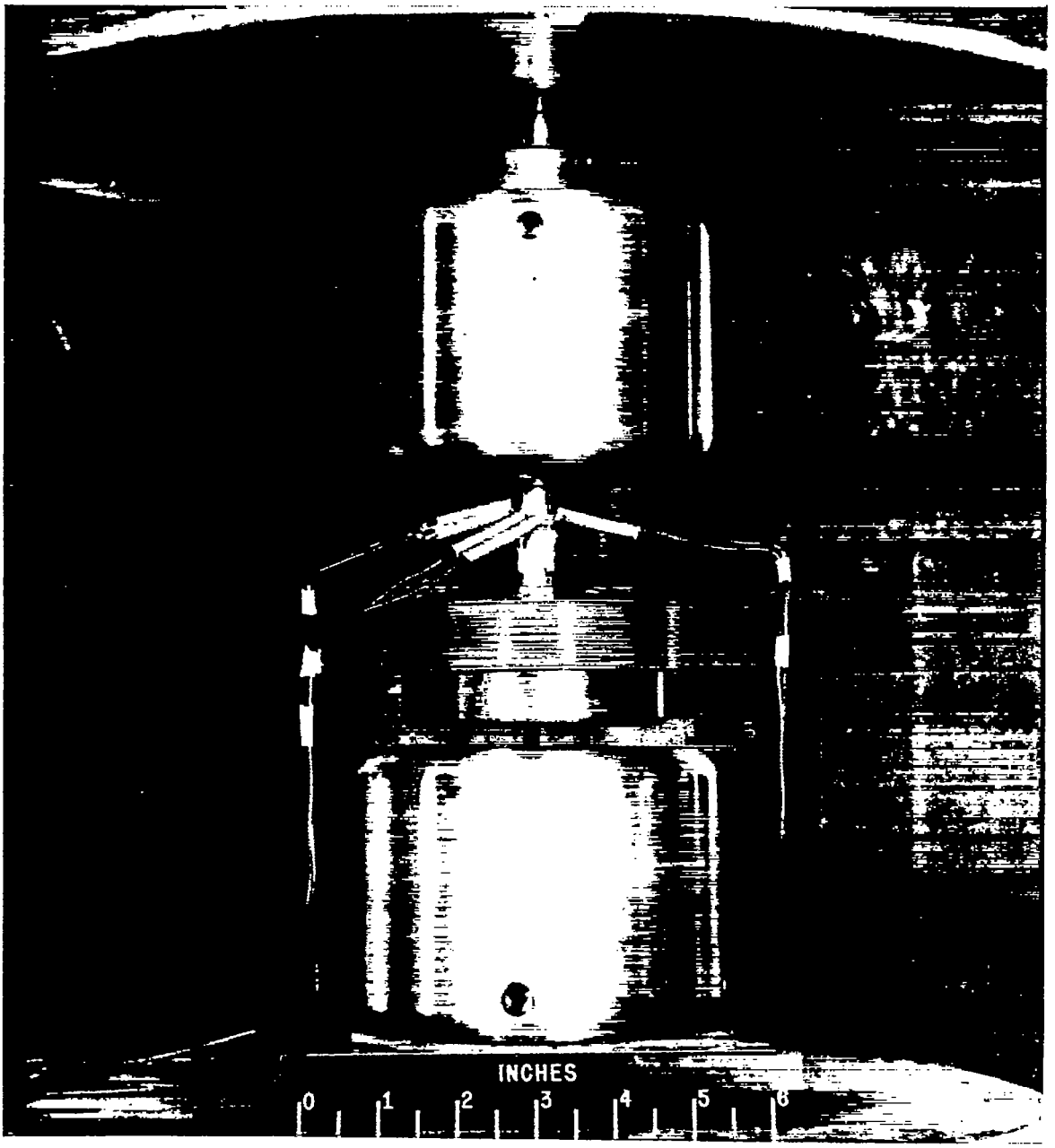

L-80886.1

Figure 3.–Tension–test setup.

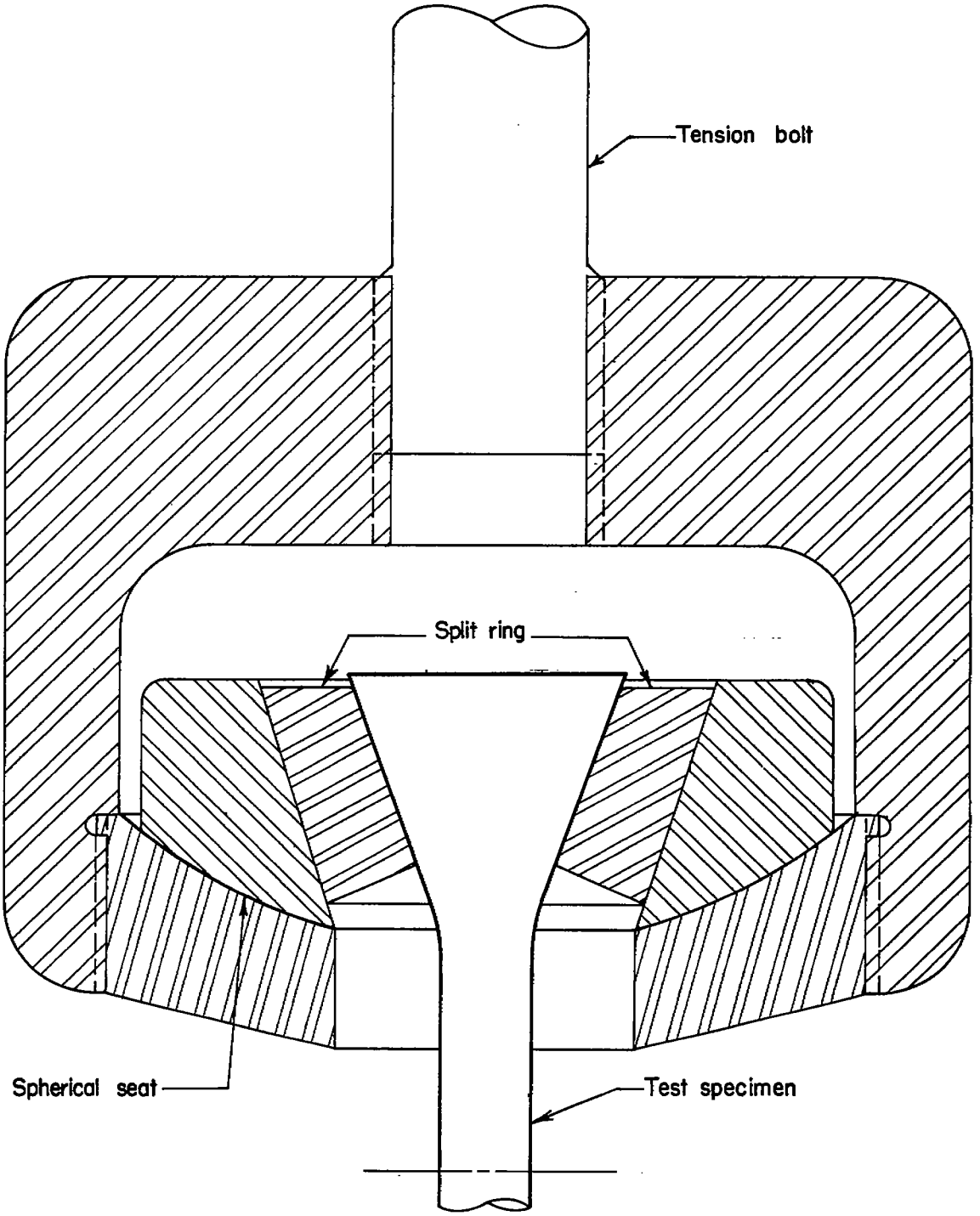

Figure 4.—Tension-test fixture.

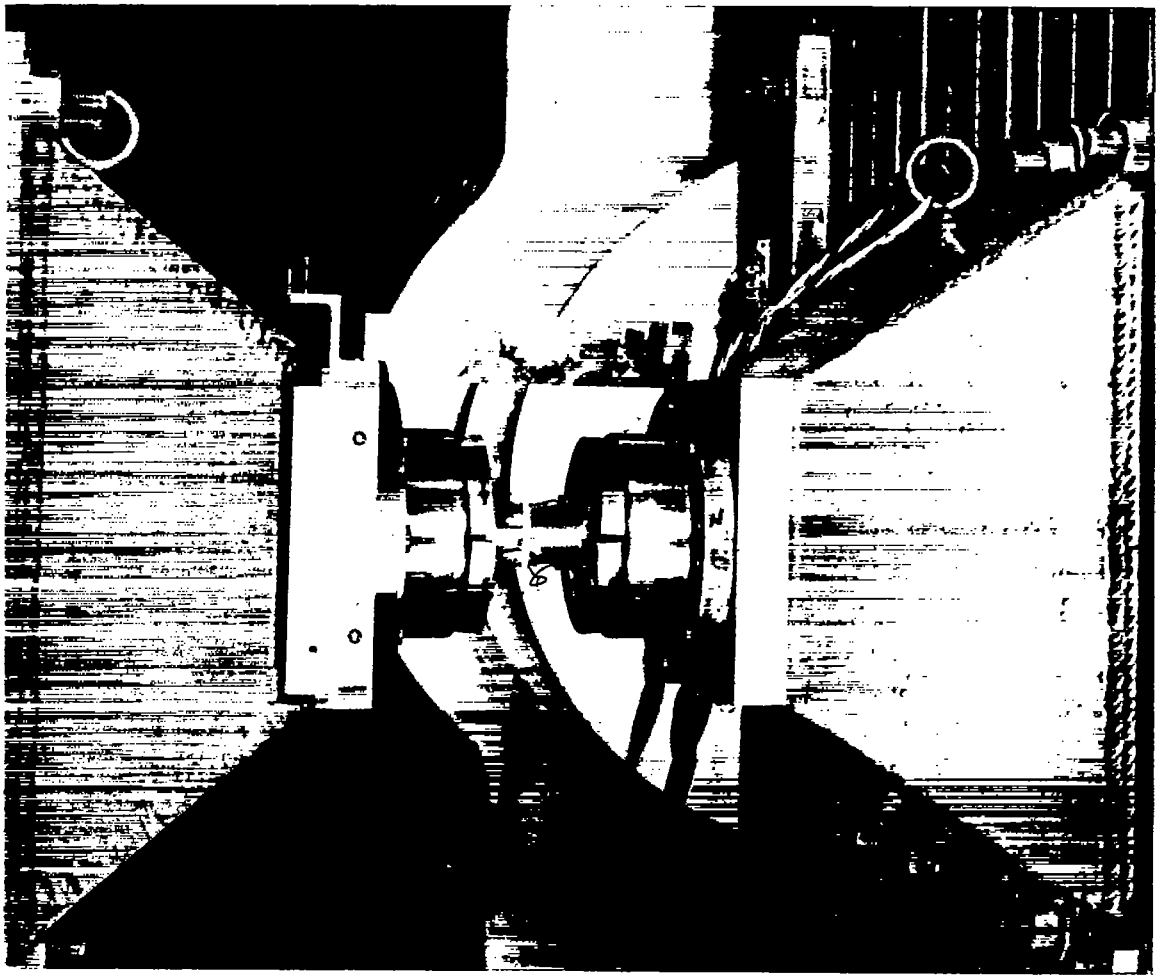

Figure 5.—Shear-test setup. L-75972

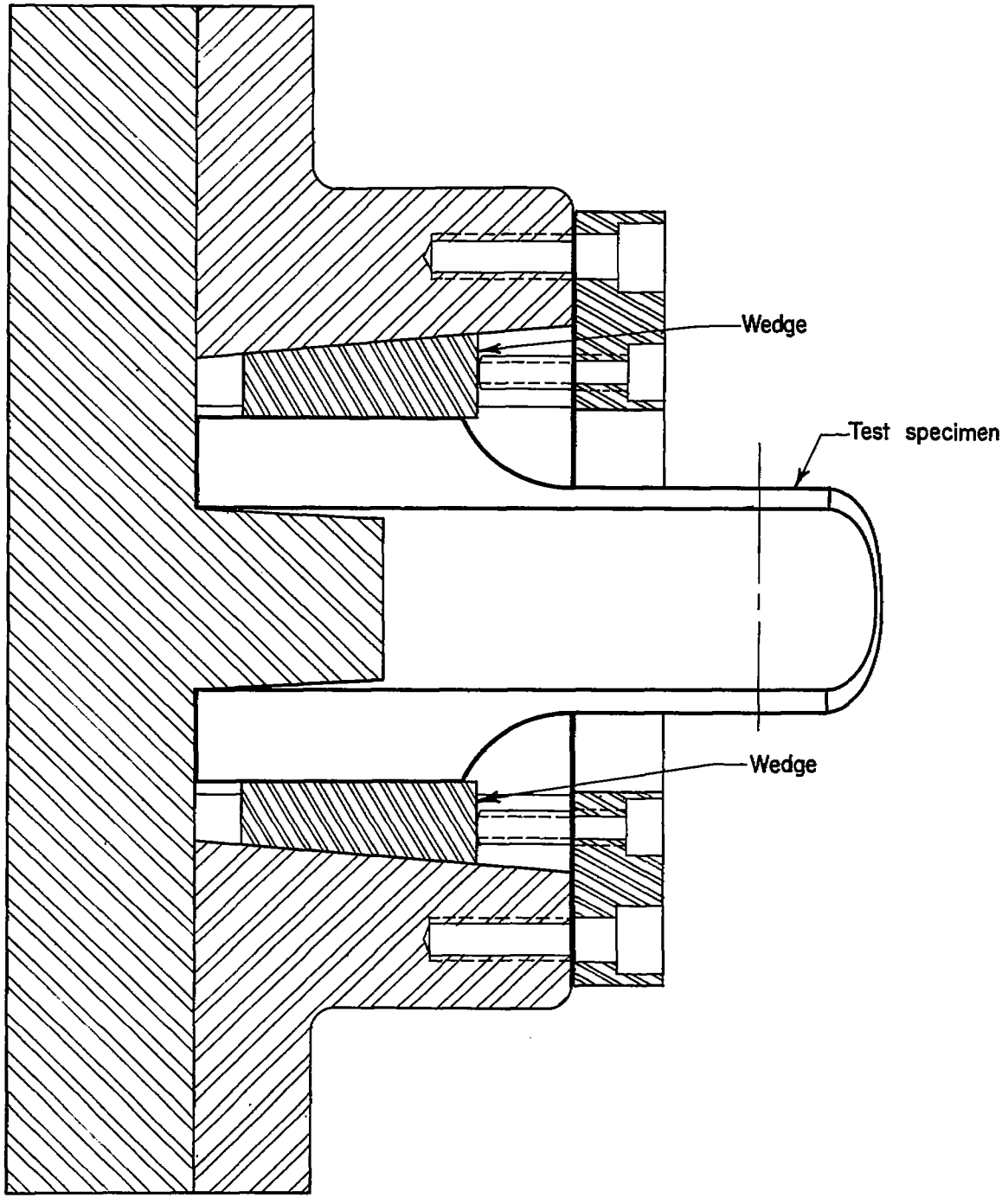

Figure 6.–Shear-test fixture.

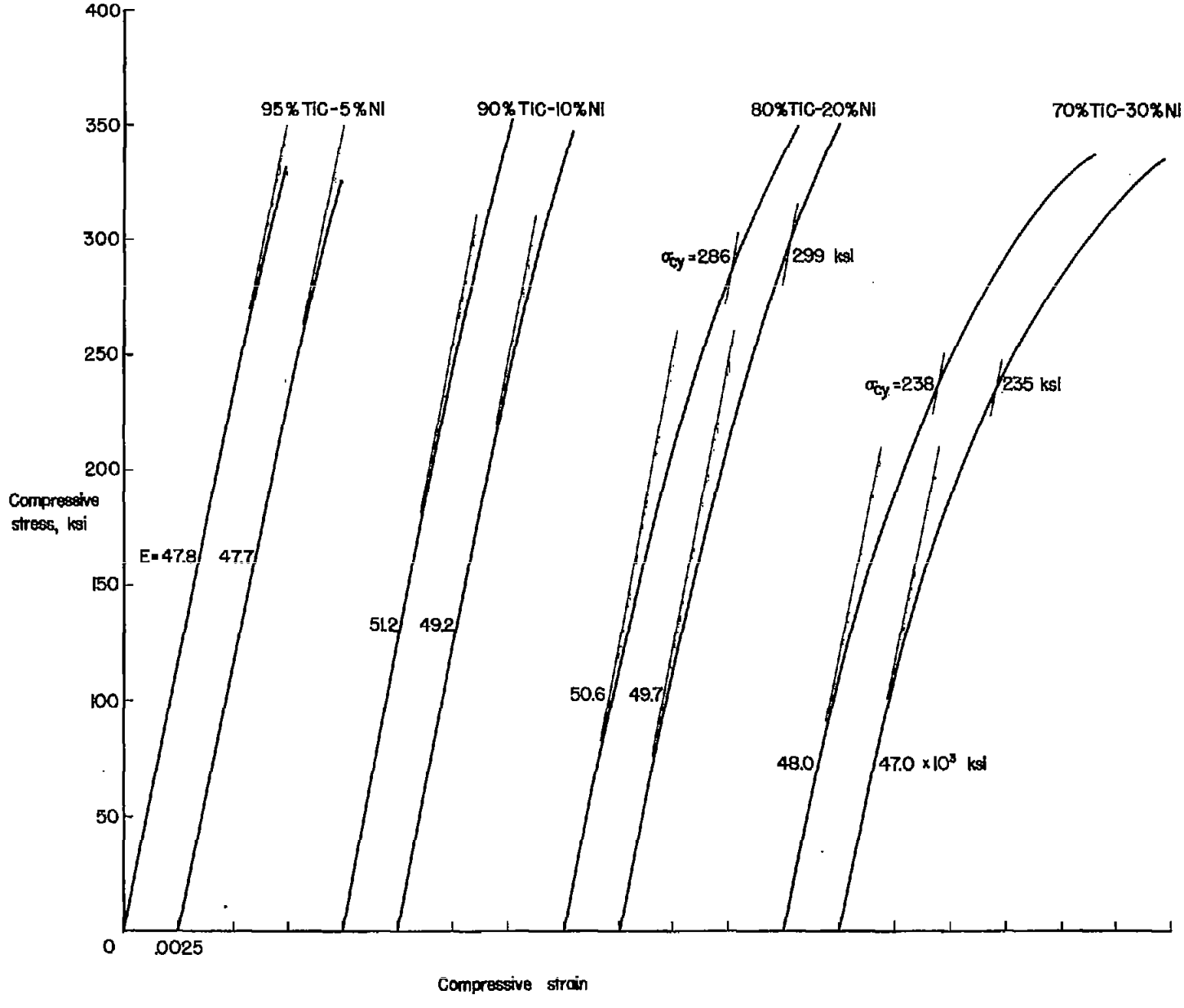

Figure 7.- Compressive stress-strain curves.

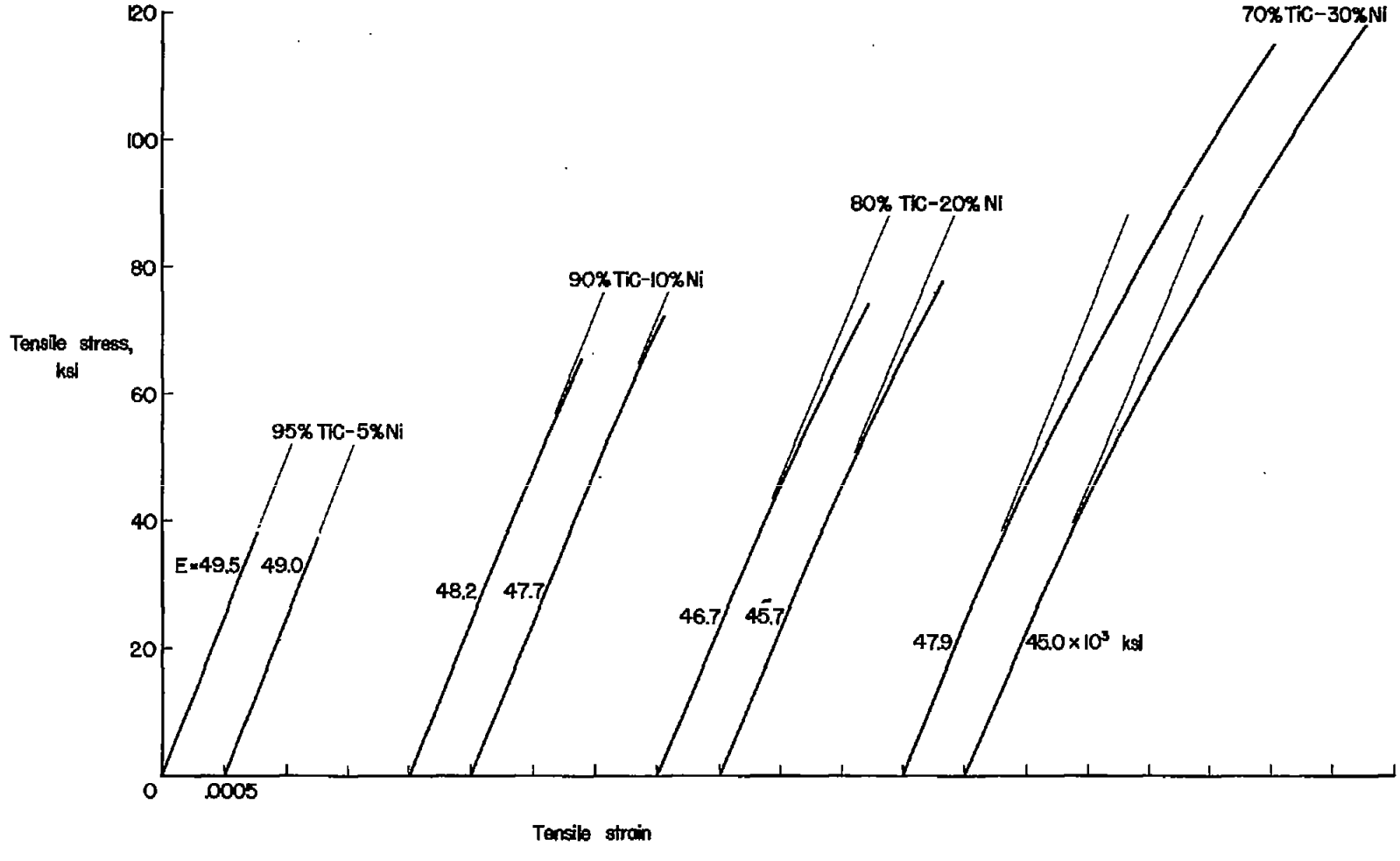

Figure 8. – Tensile stress-strain curves.

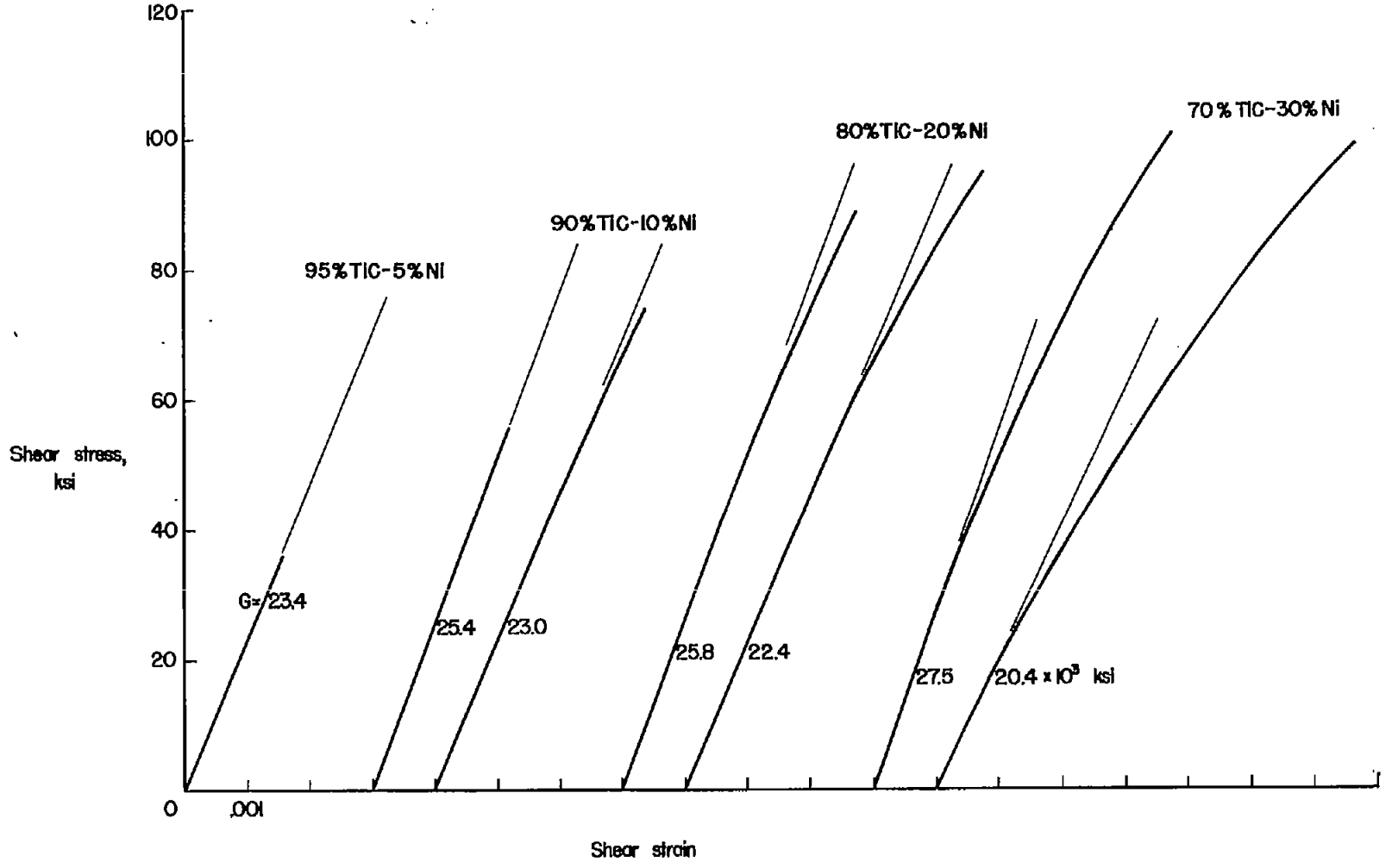

Figure 9.—Shear stress-strain curves.

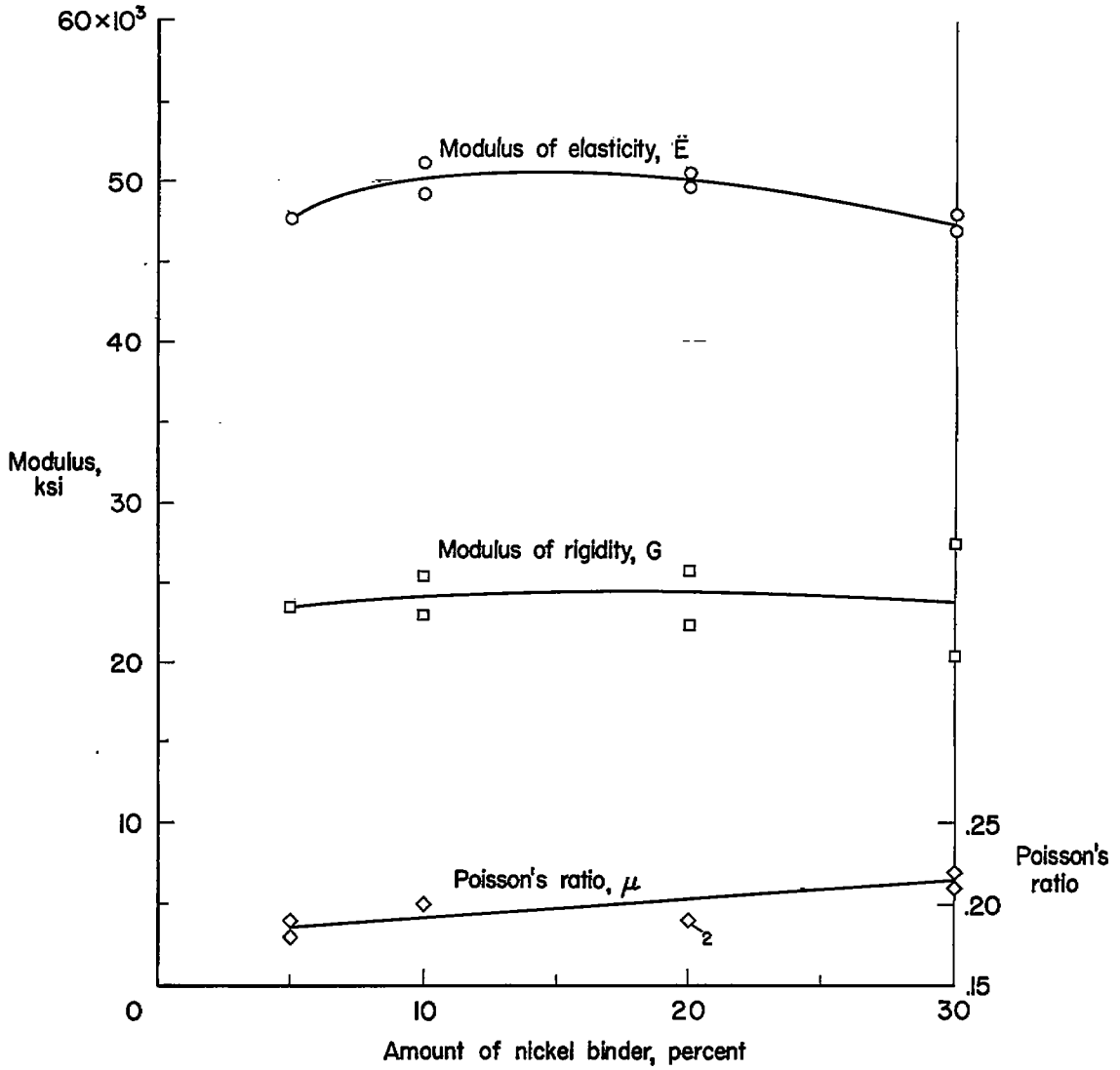

Figure 10.– Effect of amount of binder material on elastic moduli and Poisson's ratio.

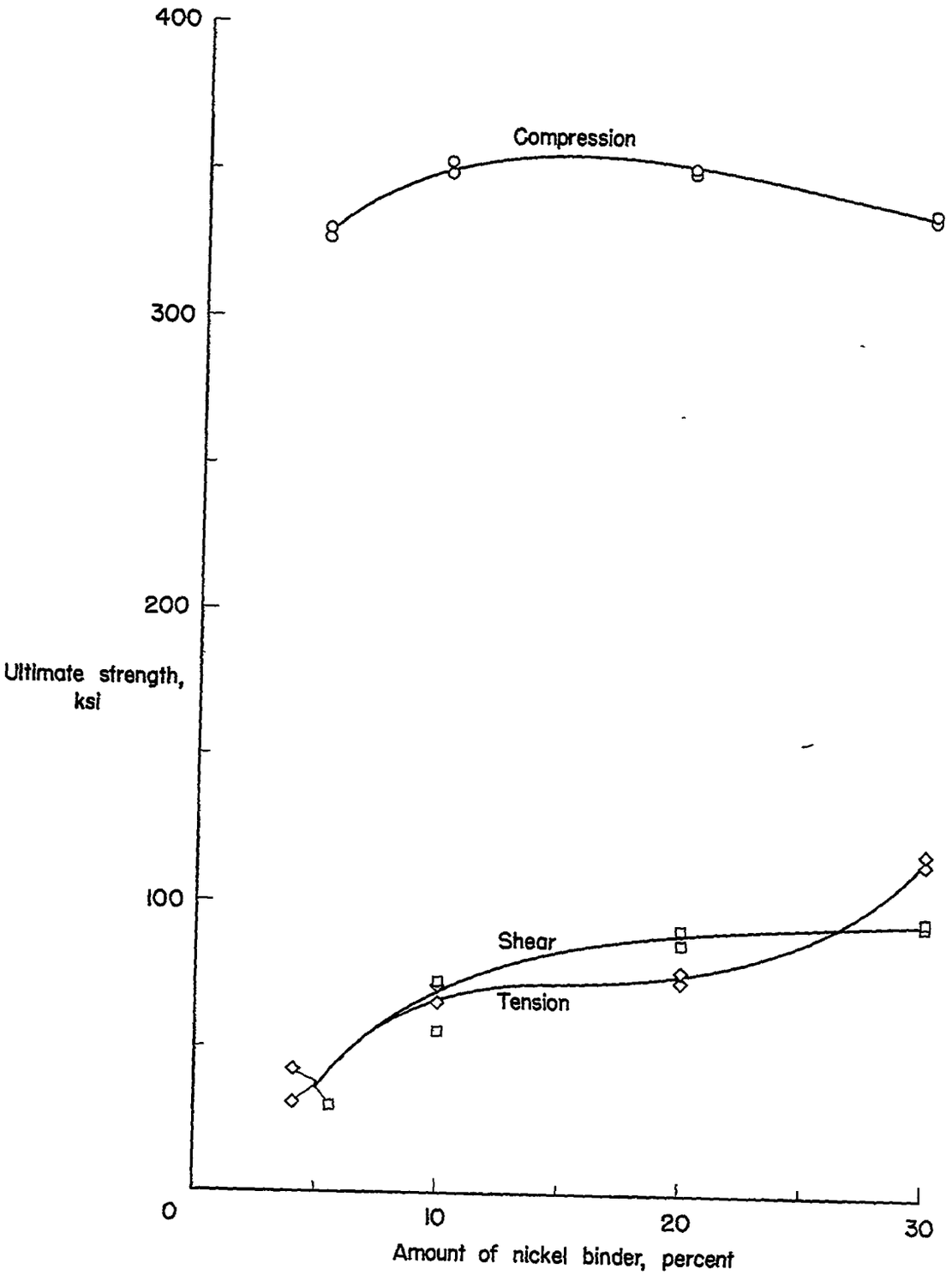

Figure 11.- Effect of amount of binder material on ultimate strength.

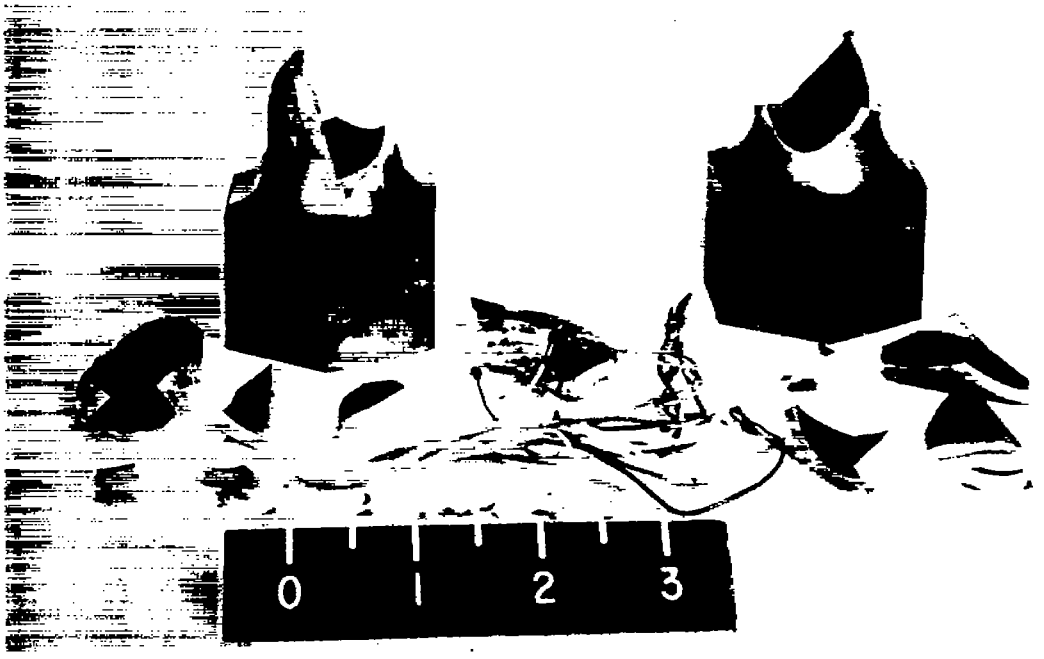

Figure 12.–Shear specimen after failure. L-75370

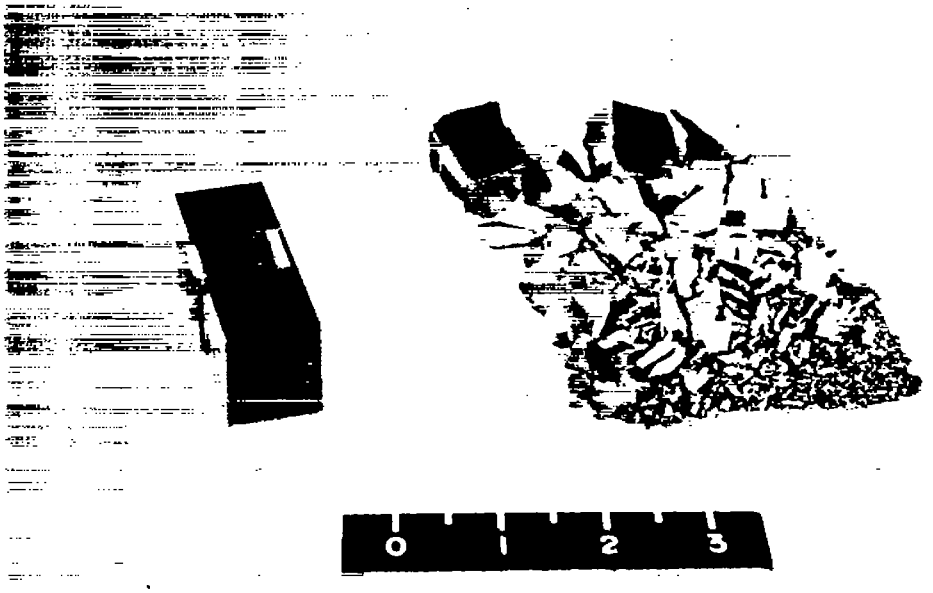

Figure 13.–Compression specimens before and after failure. L-74510